



# Solution and solid-state study of the structure of azo-coupling products from isomeric enaminones possessing *tert*-butyl group: An unprecedented observation of pure hydrazo form in azo coupled *N*-alkyl $\beta$ -enaminones

Petr Šimůnek<sup>a,\*</sup>, Zdeňka Padělková<sup>b</sup>, Vladimír Macháček<sup>a</sup>

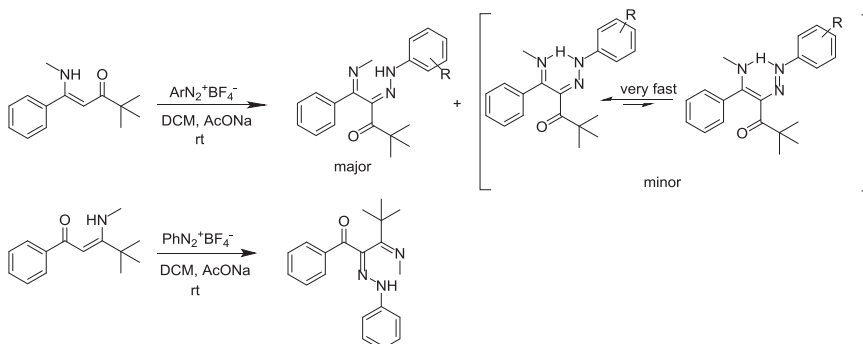
<sup>a</sup> University of Pardubice, Faculty of Chemical Technology, Institute of Organic Chemistry and Technology, Studentská 573, CZ-532 10 Pardubice, Czech Republic

<sup>b</sup> University of Pardubice, Faculty of Chemical Technology, Department of General and Inorganic Chemistry, Studentská 573, CZ-532 10 Pardubice, Czech Republic

## HIGHLIGHTS

- Isomeric azo coupled  $\beta$ -enaminones with *tert*-butyl group were synthesized.
- *tert*-Butyl group prevents conjugation in heterodiene system  $\text{N}=\text{C}-\text{C}=\text{N}-\text{N}$ .
- Pure hydrazo forms in azo coupled *N*-alkylenaminones was observed.

## GRAPHICAL ABSTRACT



## ARTICLE INFO

### Article history:

Received 21 March 2014  
Received in revised form 23 June 2014  
Accepted 23 June 2014  
Available online 30 June 2014

### Keywords:

$\beta$ -enaminones  
Azo coupling  
Azo-hydrazone tautomerism  
<sup>15</sup>N NMR  
X-ray  
Hydrogen bonds

## ABSTRACT

The structure of the azo-coupling products from enaminones derived from 4,4-dimethyl-1-phenylpentane-1,3-dione has been studied by means of solution-state <sup>1</sup>H, <sup>13</sup>C and <sup>15</sup>N NMR spectroscopy and X-ray diffractometry. The presence of bulky *tert*-butyl group hinders or even prevents from the formation of planar conjugated heterodiene system  $\text{H}-\text{N}=\text{C}=\text{C}=\text{N}=\text{N}$  with an intramolecular hydrogen bond  $\text{N}-\text{H}\cdots\text{N}=\text{N}$  which is the prerequisite for fast tautomeric exchange imino-hydrazo – enamino-azo. The minor amount of azo compounds is formed by a proton exchange through a hydrogen bond  $\text{N}-\text{H}\cdots\text{N}$ , which is either intramolecular (in solution) or intermolecular (solid state). The intermolecular exchange proceeds via the dimers of the azo coupling products. This is unprecedented result among the similar molecules hitherto studied.

© 2014 Elsevier B.V. All rights reserved.

## Introduction

Azo-hydrazone tautomerism belongs among the equilibria being very fast on NMR time scale. That means the mixture of both

the tautomers behaves spectrally as the single compound and gives only one set of signals in <sup>1</sup>H, <sup>13</sup>C and <sup>15</sup>N NMR spectra. This set is a weighted average from the individual tautomers. The proportion of the individual tautomers should be estimated from this single set of signals (mathematically one equation for two unknowns). Spectra containing the signals of both the tautomers have never been hitherto observed under any conditions. The question of

\* Corresponding author. Tel.: +420 466 037 039; fax: +420 466 037 068.

E-mail address: [petr.simunek@upce.cz](mailto:petr.simunek@upce.cz) (P. Šimůnek).

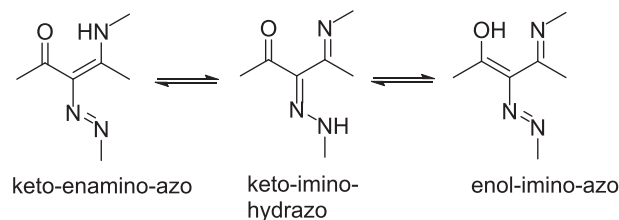
determining the equilibrium constant  $K_T$  for azo-hydrazone tautomerism for the products of azo coupling of benzenediazonium with phenols, naphthols and aromatic amines has been successfully solved by means of  $^{15}\text{N}$  NMR spectroscopy in solution ( $\text{CDCl}_3$ ). The parameters relevant for the determining of the constant are either  $\delta(^{15}\text{N})$  of the nitrogens of the tautomeric groups or the values of the coupling constants  $^1J(^{15}\text{N}-^1\text{H})$  [1–6]. Even this method, however, cannot be considered as fully exact as the results depend on the choice of standards, but more precise results are probably impossible to be obtained using any other method. More precise evaluation of the equilibrium for the azo coupling products with diazonium ions other than benzenediazonium is also not possible, as the substitution on the diazonium ion affects both the position of the tautomeric equilibrium [7] and the chemical shifts of the nitrogens through the substitution effect [8] and the corresponding  $^{15}\text{N}$  NMR parameters for potential standards have not been hitherto systematically studied. Qualitatively it is known that electron-donating substituents on the diazonium ion ( $\text{NMe}_2$ ,  $\text{OMe}$ ,  $\text{Me}$ ) increase the amount of the azo form whereas electron-withdrawing ones ( $\text{NO}_2$ ) increase the amount of the hydrazone form [7]. To what extent is the methodology using  $^{15}\text{N}$  NMR parameters applicable to the determination of the tautomeric equilibrium for the aliphatic azo coupling products, as long as the products can undergo the tautomeric rearrangement, was not quite clear although  $^{15}\text{N}$  NMR data has already been used for this purpose [9,10]. Another approach to study azo-hydrazone tautomerism is theoretical, by means of quantum chemistry calculations (from many examples e.g. [11,12]. AM 1 Geometry optimization was also used for structural studies on some azo coupled enaminones [13].

In the case of the products of azo coupling on aliphatic substrates it has been said up to now in the literature [14,15] that there does not exist azo form in the cases where the tautomeric rearrangement to hydrazone form is possible.

When the reaction is carried out on a compound  $\text{X}-\text{CHY}-\text{Z}$ , the azo form does not have a hydrogen that can lead to the tautomerism. When at least one of the substituents ( $\text{X}$ ,  $\text{Y}$ ,  $\text{Z}$ ) at the quaternary centrum is acyl ( $\text{R}-\text{C}=\text{O}$ ) then the product in this case is also hydrazone and not azo compound. In fact, compounds type **1** are seldom isolable and undergo Japp–Klingemann reaction to give the corresponding hydrazones **2** [15–17] (Scheme 1).

From the tautomeric point of view the major attention in the literature has been devoted to the products of azo coupling with  $\beta$ -enaminones [9,10,18–27]. These products contain three potentially tautomeric groups and can theoretically exist in several tautomeric forms (Scheme 2): keto-enamino-azo, keto-imino-hydrazo and enol-imino-azo.

During the past several years we have accomplished relatively extensive survey how the structure of both the starting  $\beta$ -enaminone and diazonium salt affects the structure of the azo coupling products including the position of the tautomeric equilibrium [9,10,18–27]. The results obtained are summarized in the review [26]. It can be stated that the study of the azo coupled enaminones constitutes a complex problem with a number of variables (structures both the substrate and diazonium salt, solvent, ...). Among the results following from the studies is the fact that a number of the azo coupled enaminones exist to less or more extent as azo compounds. The discovery, that even the products of the azo



**Scheme 2.** Possible tautomeric forms of the azo coupled  $\beta$ -enaminones.

coupling to aliphatic substrates can exist as stable azo compounds (although the rearrangement into the hydrazone form is possible), are contradiction of still existing opinion [14,15].

The results obtained during the study of azo coupling on isomeric enaminones derived from benzoylacetone [22] indicate the possibility of steric effects on the structure of the products. The effects were significant and comprised both the affecting the position of the tautomeric equilibrium and *E/Z* isomerism and the kind of hydrogen bonding. In some cases a small change of the structure of the enaminone led to quite different products [28].

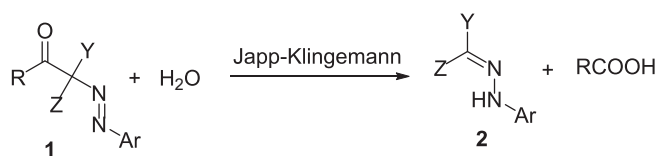
In the present work we are dealing with the study of the structure of the azo coupling products on some sterically hindered enaminones containing *tert*-butyl group both in solution and in solid state. An introduction of a *tert*-butyl group generally causes an increasing the steric tension in the molecule and represents a convenient model for this kind of studies.

## Experimental

### Methods

NMR data were obtained in  $\text{CDCl}_3$  using Bruker AVANCE III spectrometer operating at 400.13 MHz ( $^1\text{H}$ ), 100.62 ( $^{13}\text{C}$ ) and 40.55 MHz ( $^{15}\text{N}$ ) equipped with 5 mm broad-band probe having magnetic field gradients in *z*-direction. All the pulse programs were taken from the Bruker sequence library. The spectra were calibrated on internal TMS ( $^1\text{H}$ ,  $\delta = 0.00$  ppm), the middle signal of the solvent multiplet ( $^{13}\text{C}$ ,  $\delta = 77.0$  ppm) and on external neat  $\text{CH}_3^{15}\text{NO}_2$  placed in a coaxial capillary ( $^{15}\text{N}$ ,  $\delta = 0.0$ ), resp.  $^{13}\text{C}$  NMR spectra were measured in a standard way using broadband proton decoupling.  $^{15}\text{N}$  Chemical shifts (Table 1) were obtained by an indirect detection using both 2D  $^1\text{H}-^{15}\text{N}$  HMBC and 2D  $^1\text{H}-^{15}\text{N}$  HMQC pulse sequences. The HMBC measurements were optimized on  $^1J(^1\text{H}, ^{15}\text{N}) = 90$  Hz and long-range  $^1\text{H}, ^{15}\text{N}$  couplings 3.5 Hz. The HMQC sequence was optimized on one-bond coupling 90 Hz. The gradient ratios for both the sequences were 70:30:50.1, time domain  $4\text{ k} \times 128$ , sine-bell windowing in both dimensions. The values of  $^1J(^1\text{H}, ^{15}\text{N})$  were read either at natural abundance using 1D  $^1\text{H}-^{15}\text{N}$  HMBC pulse sequence or from satellites in proton spectra (in the case of  $^{15}\text{N}$  enriched samples **3a** and **4**). 2D NOESY spectra were measured in States-TPPI acquisition mode, mixing time 800 ms, time-domain  $2\text{ k} \times 128$  zero-filled to  $2\text{ k} \times 1\text{ k}$ , QSINE multiplication in both dimensions, relaxation delay set to 2 s, number of dummy scans 16, 88 scans per *t*<sub>1</sub> increment. The phasing was carried giving negative diagonal peaks.

The X-ray data (Table 2) for crystals of **3a–d** and **4** were obtained at 150 K using Oxford Cryostream low-temperature device on a Nonius Kappa CCD diffractometer with Mo  $\text{K}\alpha$  radiation ( $\lambda = 0.71073$  Å), a graphite monochromator, and the  $\phi$  and  $\chi$  scan mode. Data reductions were performed with DENZO-SMN [29]. The absorption was corrected by integration methods [30]. Structures were solved by direct methods (Sir92) [31] and refined by full matrix least-square based on  $F^2$  (SHELXL97) [32]. Hydrogen atoms were mostly localized on a difference Fourier map, however



**Scheme 1.** The fate of the acyl-substituted aliphatic azo compounds.

**Table 1**<sup>15</sup>N NMR data for compounds **3** and **4** in CDCl<sub>3</sub>.

	R	δ( <sup>15</sup> N <sub>α</sub> )	δ( <sup>15</sup> N <sub>β</sub> )	δ( <sup>15</sup> N <sub>γ</sub> )	<sup>1</sup> J( <sup>15</sup> N <sub>α</sub> , <sup>1</sup> H)(Hz)	δ <sup>1</sup> H(NH)	A/B ratio
<b>3aA</b>	H	−237	−35	<sup>a</sup>	92	8.05 <sup>b</sup>	4/1
<b>3aB</b>		−172	−5	<sup>a</sup>	71	14.87	
<b>3bA</b>	4-F	−239	−34	−57	93	8.05 <sup>b</sup>	2/1
<b>3bB</b>		−127	<sup>a</sup>	<sup>a</sup>	48	14.74	
<b>3cA</b>	4-OMe	−238	−34	−57	93	8.03 <sup>b</sup>	2/1
<b>3cB</b>		<sup>a</sup>	<sup>a</sup>	<sup>a</sup>	41	14.60	
<b>3dA</b>	3-CF <sub>3</sub>	−239	−37	−54	93	8.06 <sup>b</sup>	2/1
<b>3dB</b>		−166	<sup>a</sup>	<sup>a</sup>	61	14.93	
<b>4</b>	H	−235	−34	<sup>a</sup>	92	7.77 <sup>b</sup>	

<sup>a</sup> Not detected.<sup>b</sup> Concentration-dependent value (for 20 mg/0.6 mL of the solvent shown).

to ensure uniformity of treatment of crystal, all hydrogen were recalculated into idealized positions (riding model) and assigned temperature factors  $H_{iso}(H) = 1.2 U_{eq}(\text{pivot atom})$  or of  $1.5 U_{eq}$  for the methyl moiety with  $C-H = 0.96$  and  $0.93 \text{ \AA}$  for methyl and hydrogen atoms in aromatic ring, respectively. In all compounds **3** the difference Fourier map showed diffuse electron density between nitrogen atoms with two maxima from which two proton positions could be identified. Refinement of the two tautomeric H atoms with partial occupancy and isotropic thermal parameters fixed at 1.2 times the average of those of the related nitrogen atoms was successfully attempted giving the final occupancy factors in the range 69–81% for H1 and 31–19% for H3 for compounds **3a–3d**. The CF<sub>3</sub> group in **3d** is disordered and the disorder was treated/split to two positions with standard methods implemented in SHELXL97 [32]. The major tautomer is refined in cases of all compounds.

Elemental analyses were performed with a Flash 2000 CHNS Elemental Analyzer. Melting points were measured with a Kofler hot-stage microscope Boetius PHMK 80/2644 and were not corrected. Mass spectra were measured with a high-resolution MALDI mass spectrometer LTQ Orbitrap XL (Thermo Fisher Scientific, Bremen) equipped with a nitrogen UV laser (337 nm, 60 Hz). The LTQ Orbitrap instrument was operated in the positive ion mode over a

normal mass range ( $m/z$  50–2000). The used matrix was *trans*-2-[3-(4-*tert*-butylphenyl)-2-methylprop-2-en-1-ylidene]malononitrile (DCTB). Mass spectra were averaged over the whole MS record for all measured samples.

### Material

All the solvents and reagents were obtained from commercial sources and were used without further purification. Diazonium tetrafluoroborates were prepared according to a standard procedure [19]. 4,4-Dimethyl-1-phenylpentane-1,3-dione (**1**) was obtained commercially (Alfa Aesar). Compounds **2–4** were prepared using the protocol published in [27]. <sup>15</sup>N enriched compounds were prepared from double <sup>15</sup>N labelled diazonium tetrafluoroborate according to the protocol published in [27]. Diazonium salt  $2 \times ^{15}\text{N}$  was prepared in an ordinary way from <sup>15</sup>N aniline and <sup>15</sup>N sodium nitrite.

Data for compounds **3b–d** were published in [27].

Characterization of newly prepared compounds:

### 3-Methylamino-4,4-dimethyl-1-phenylpent-2-en-1-one (**2b**)

Compound obtained as the by-product (yield 11%) from the reaction of **1** with ethanolic methylamine according to the

**Table 2**Crystallographic data for compounds **3a–d** and **4**.

	<b>3a</b>	<b>3b</b>	<b>3c</b>	<b>3d</b>	<b>4</b>
Empirical formula	C <sub>20</sub> H <sub>23</sub> N <sub>3</sub> O	C <sub>20</sub> H <sub>22</sub> FN <sub>3</sub> O	C <sub>21</sub> H <sub>25</sub> N <sub>3</sub> O <sub>2</sub>	C <sub>21</sub> H <sub>22</sub> F <sub>3</sub> N <sub>3</sub> O	C <sub>20</sub> H <sub>23</sub> N <sub>3</sub> O
M	321.41	339.41	351.44	389.42	321.41
Crystal system	Monoclinic	Monoclinic	Orthorhombic	Orthorhombic	Monoclinic
Space group	<i>P</i> 2 <sub>1</sub> / <i>c</i>	<i>P</i> 2 <sub>1</sub> / <i>c</i>	<i>P</i> 2 <sub>1</sub> 2 <sub>1</sub> 2 <sub>1</sub>	<i>Pbca</i>	<i>P</i> 2 <sub>1</sub> / <i>c</i>
<i>a</i> (Å)	10.1150(8)	10.1830(5)	10.8740(10)	12.6170(9)	12.8310(14)
<i>b</i> (Å)	10.1100(5)	10.3400(6)	17.5772(18)	17.374(2)	22.213(2)
<i>c</i> (Å)	19.5181(11)	19.4861(12)	20.1730(14)	18.614(2)	12.3770(10)
β (°)	114.553(5)	115.994(5)	90	90	94.434(7)
<i>V</i> (Å <sup>3</sup> )	1815.5(2)	1844.2(2)	3855.8(6)	4080.3(7)	3517.1(6)
<i>Z</i>	4	4	8	8	8
<i>D<sub>c</sub></i> (g cm <sup>−3</sup> )	1.176	1.222	1.211	1.268	1.214
Crystal size (mm)	0.59 × 0.46 × 0.27	0.48 × 0.31 × 0.26	0.27 × 0.25 × 0.16	0.38 × 0.26 × 0.23	0.30 × 0.25 × 0.24
μ (mm <sup>−1</sup> )	0.074	0.084	0.079	0.098	0.076
<i>F</i> (000)	688	720	1504	1632	1376
<i>h</i> ; <i>k</i> ; <i>l</i> range	−11, 13; −11, 13; −25, 25	−13, 13; −13, 12; −25, 23	−11, 13; −22, 22; −24, 26	−16, 15; −22, 20; −24, 23	−16, 16; −28, 28; −16, 16
θ range (°)	2.86; 27.48	2.81; 27.50	2.75; 26.50	2.96; 27.50	2.39; 27.50
Reflections measured	15,017	13,056	26,787	28,226	54,753
– independent ( <i>R</i> <sub>int</sub> ) <sup>a</sup>	4093 (0.0304)	4191 (0.0363)	8353 (0.0511)	4620 (0.0306)	7962 (0.0465)
– observed [ <i>I</i> > 2σ( <i>I</i> )]	3154	3129	6387	3352	5541
Parameters refined	4093	226	469	281	433
Max/min Δρ (e Å <sup>−3</sup> )	0.277/−0.255	0.288/−0.286	0.236/−0.231	0.299/−0.202	0.296/−0.281
GOF <sup>b</sup>	1.115	1.083	1.187	1.121	1.121
<i>R</i> <sup>c</sup> / <i>wR</i> <sup>c</sup>	0.0500/0.1070	0.0523/0.1095	0.0518/0.0966	0.0494/0.1003	0.0593/0.1085

<sup>a</sup>  $R_{int} = \sum |F_o^2 - F_c^2| / \sum F_o^2$ .<sup>b</sup> GOF =  $[\sum (w(F_o^2 - F_c^2)^2) / (N_{diffs} - N_{params})]^{1/2}$  for all data.<sup>c</sup>  $R(F) = \sum ||F_o| - |F_c|| / \sum |F_o|$  for observed data,  $wR(F^2) = [\sum (w(F_o^2 - F_c^2)^2) / (\sum w(F_o^2)^2)]^{1/2}$  for all data.

published procedure [22] with **2a** as the main product. The structure of the products has been verified by means of  $^1\text{H}$ – $^{13}\text{C}$  HMBC [27]. The compound **2b** contained ca 11% of **2a**.

$^1\text{H}$  NMR  $\delta$ : 1.38 (s, 9H); 3.23 (d,  $J$  = 5.7 Hz, 3H); 5.84 (s, 1H); 7.36–7.44 (m, 3H); 7.83–7.85 (m, 2H); 12.24 (brs, 1H).

#### 2,2-Dimethyl-5-methylimino-5-phenyl-4- $^{15}\text{N}_2$ ]phenylhydrazonopentane-3-one (**3a**)

Obtained by the reaction of **2a** with benzenediazonium tetrafluoroborate ( $2 \times ^{15}\text{N}$ ). Column chromatography silica/DCM–EtOAc 20:1 v/v, yield 74%, m.p. 176–179 °C. Product is ca 4:1 mixture of isomers. Anal. calcd. for  $\text{C}_{20}\text{H}_{23}\text{N}_3\text{O}$ : C 74.30, H 7.17, N 13.59. Found C 74.32, H 7.35, N 13.32.

HRMS (MALDI) calcd. for  $\text{C}_{20}\text{H}_{24}\text{N}_3\text{O}$   $[\text{M} + \text{H}]^+$  324.18546, found 324.18549; for  $\text{C}_{20}\text{H}_{23}\text{N}_3\text{NaO}$   $[\text{M} + \text{Na}]^+$  346.16740, found 346.16779; for  $\text{C}_{20}\text{H}_{23}\text{N}_3\text{K}_3\text{O}$   $[\text{M} + \text{K}]^+$  362.14134, found 362.14184.

$^1\text{H}$  NMR major form  $\delta$  (ppm): 1.51 (s, 9H); 3.26 (s, 3H); 7.02–7.04 (m, 1H); 7.15–7.18 (m, 2H); 7.31–7.42 (m, 5H); 7.62–7.65 (m, 2H); 8.05 (d,  $J(^1\text{H}, ^{15}\text{N})$  = 92.3 Hz, 1H).

$^1\text{H}$  NMR minor form  $\delta$  (ppm): 1.31 (s, 9H); 3.16 (s, 3H); 7.08–7.10 (m, 1H); 7.13–7.15 (m, 2H); 7.31–7.42 (m, 7H); 14.87 (d,  $J(^1\text{H}, ^{15}\text{N})$  = 72.6 Hz, 1H).

$^{13}\text{C}$  NMR major form  $\delta$  (ppm): 28.0; 41.2; 44.2; 114.2 (t,  $J$  = 1.9 Hz); 122.9; 126.6; 129.0; 129.6 (d,  $J(^{13}\text{C}, ^{15}\text{N})$  = 1.9 Hz); 131.1; 135.6; 137.4 (d,  $J(^{13}\text{C}, ^{15}\text{N})$  = 3.4 Hz); 142.5 (dd,  $J(^{13}\text{C}, ^{15}\text{N})$  = 19.2 Hz, 6.0 Hz); 163.6; 201.4 (dd,  $J(^{13}\text{C}, ^{15}\text{N})$  = 10.6 Hz, 4.4 Hz).

$^{13}\text{C}$  NMR minor form  $\delta$  (ppm): 28.3; 37.6; 43.8; 116.2 (br t); 123.9; 126.8; 128.2; 128.4; 129.3 (br d,  $J(^{13}\text{C}, ^{15}\text{N})$  = 1.6 Hz); 133.7; 135.0; 145.3 (dd,  $J(^{13}\text{C}, ^{15}\text{N})$  = 14.4 Hz, 6.2 Hz); 166.8; 204.8 (dd,  $J(^{13}\text{C}, ^{15}\text{N})$  = 10.5 Hz, 3.1 Hz).

#### 4,4-Dimethyl-3-methylimino-1-phenyl-2- $^{15}\text{N}_2$ ]phenylhydrazonopentane-1-one (**4**)

Obtained by the reaction of **2b** with benzenediazonium tetrafluoroborate ( $2 \times ^{15}\text{N}$ ). Column chromatography silica/DCM–EtOAc 20:1 v/v, pale yellow solid, yield 67%, m.p. 145–150 °C. Anal. calcd. for  $\text{C}_{20}\text{H}_{23}\text{N}_3\text{O}$ : C 74.30, H 7.17, N 13.59. Found C 74.35, H 7.37, N 13.30.

HRMS (MALDI) calcd. for  $\text{C}_{20}\text{H}_{24}\text{N}_3\text{O}$   $[\text{M} + \text{H}]^+$  324.18546, found 324.18547.

$^1\text{H}$  NMR  $\delta$  (ppm): 1.23 (s, 9H); 3.16 (s, 3H); 7.00–7.07 (m, 3H); 7.28–7.32 (m, 2H); 7.49–7.53 (m, 2H); 7.58–7.62 (m, 1H); 7.77 (dd,  $J$  = 91.7 Hz; 2.5 Hz, 1H); 8.06–8.09 (m, 2H).

$^{13}\text{C}$  NMR  $\delta$  (ppm): 28.2; 39.9; 41.4; 114.1 (t,  $J(^{13}\text{C}, ^{15}\text{N})$  = 1.9 Hz); 122.9; 128.0; 129.5 (d,  $J(^{13}\text{C}, ^{15}\text{N})$  = 1.6 Hz); 130.4; 132.3; 136.7; 140.4 (d,  $J$  = 3.9 Hz); 142.2 (dd,  $J$  = 19.1 Hz, 6.1 Hz); 173.0 (t, 1.3 Hz); 189.5 (dd,  $J$  = 11.5 Hz, 5 Hz).

## Results and discussion

### Synthesis

Starting  $\beta$ -enaminones **2a,b** were prepared by a condensation of the  $\beta$ -diketone **1** with ethanolic methylamine [27] (Scheme 3). Both the isomers were successfully separated by column chromatography which afforded us an opportunity to study the influences of *tert*-butyl group in comparison with phenyl group on the structure of the azo coupling products.

Azo coupling products **3, 4** were obtained by ordinary reaction of  $\beta$ -enaminones **2** with the corresponding diazonium tetrafluoroborates in DCM [19] (Scheme 3).

### The structure of the azo coupling products in $\text{CDCl}_3$ solution

The estimation of the azo-hydrazone tautomerism was done using the principles mentioned in [26].

Compounds **3a–d** are, in  $\text{CDCl}_3$  solution, a mixture of two isomers (**A/B**).

From both the values  $\delta(^{15}\text{N})$  and  $J(^{15}\text{N}, ^1\text{H})$  of the compounds **3a–d** (Table 1) it is evident that all the major forms (**A**) are pure hydrazones regardless the substitution of the starting diazonium salt. Due to the value of  $\delta(^{15}\text{N}_\beta)$  (for the designation of the individual nitrogens see Scheme 5) the absence of an intramolecular hydrogen bond can be stated [33]. This is in accordance with relatively low chemical shift of NH protons ( $\delta \sim 8$ ).

The situation in minor isomers (**B**) is quite different. Relatively high chemical shift of NH protons ( $\delta > 14$  ppm) can be accounted for the presence of an intramolecular hydrogen bond  $\text{N}=\text{H} \cdots \text{X}$  ( $\text{X}=\text{O}, \text{N}$ ). Compounds **3aB–3dB** are evidently mixtures of azo-hydrazo tautomers (see Table 1). The hydrazone content depends on the substitution of the starting diazonium salt and decreases in the order  $\text{R}=\text{H} > 3\text{-CF}_3 > 4\text{-F} > 4\text{-OMe}$ , see Scheme 5. (Please note: the order is determined on the basis of  $J(^{15}\text{N}, ^1\text{H})$  values, because the chemical shifts  $\delta(^{15}\text{N})$  for minor isomers were not obtained for all compounds). The carbonyl group in all the compounds is intact by the tautomerism (according to  $^{13}\text{C}$  NMR spectroscopy).

Compound **4** (unlike its isomer **3a**) exists in  $\text{CDCl}_3$  as one isomer only, which is, on the basis of NMR data in Table 1, pure hydrazone without intramolecular hydrogen bond.

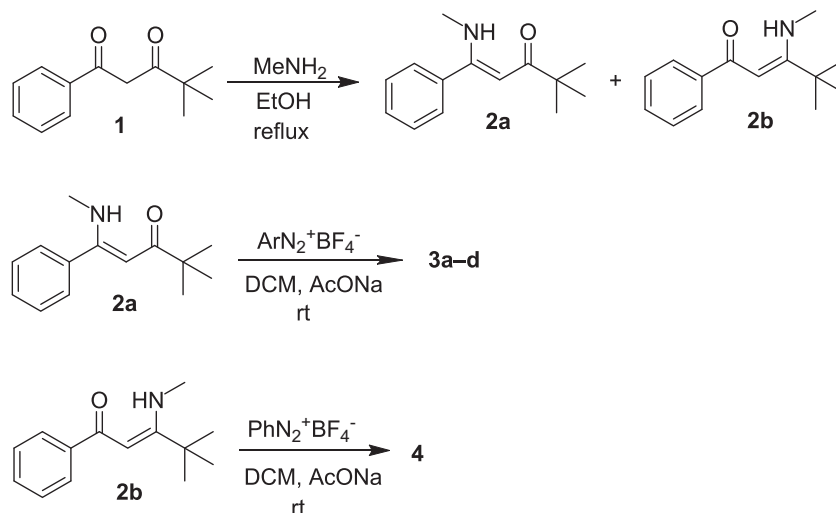
Important structural information can be extracted from the coupling constants  $J(^{13}\text{C}, ^{15}\text{N})$  (Fig. 1). Thanks to the stereochemical dependence of the  $^2J(^{13}\text{C}, ^{15}\text{N})$  value (Scheme 4, [34,35]) it can be used for determining the configuration on  $\text{C}=\text{N}=\text{NH}$  double bond. Based on the analysis of the values obtained for compounds **3aA/3aB** and **4** it can be assumed that all the compounds have *E* configuration on  $\text{C}=\text{N}=\text{NH}$  double bond (Scheme 4). It is in accordance with the crystallographic results (Figs. 6 and 7).

The NOE interaction in compound **3aA** (Fig. 2, left) reflects the spatial proximity of the  $\text{C}=\text{NCH}_3$  and  $\text{C}=\text{N}=\text{NH}$  groups. In general, on the basis of NOE interactions it can be stated that the structure of the compound **3aA** in solution is similar to the structure in the crystalline state (Fig. 6). The relative spatial proximity of *tert*-butyl and  $\text{NCH}_3$  groups indicates *Z* configuration on  $\text{C}=\text{N}-\text{CH}_3$  double bond.

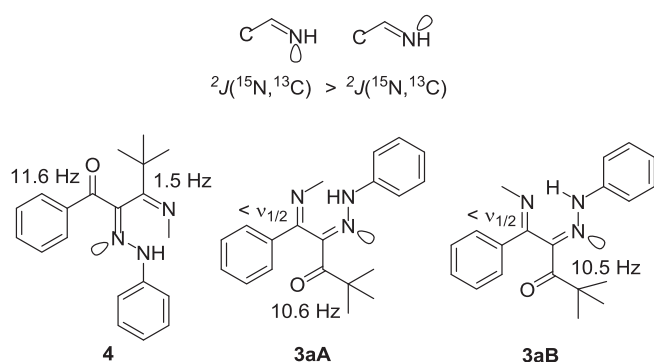
Compound **3aB** possesses, on the basis of the above-mentioned interpretations of  $^2J(^{13}\text{C}, ^{15}\text{N})$  values, an intramolecular hydrogen bonding  $\text{N}=\text{H} \cdots \text{N}=\text{C}$ . The  $\text{C}=\text{NCH}_3$  double bond of **3aB** has therefore *E* configuration. That explains why the minor isomer is, on the contrary to the major one, the mixture of azo-hydrazo tautomers. The arrangement with the hydrogen bonding enables fast proton transfer between two basic centres (Scheme 5). This is not possible, neither in **3aA** nor **4** and, hence, these compounds are pure hydrazones. The compounds **3aA/3aB** are *E/Z* isomers. The predominance of **A** isomer can be caused by steric demands of nearby groups *tert*-butyl and Ph in **B** isomer (Scheme 5).

From the NOE results obtained on compound **4** it follows that *t*Bu– $\text{C}=\text{N}-\text{CH}_3$  group is turned around the  $\text{N}=\text{C}-\text{N}$  single bond in relation to the rest of the molecule (NOE interactions of *tert*-butyl and  $\text{NCH}_3$  groups with both the benzene rings). The configuration of  $\text{C}=\text{N}-\text{CH}_3$  double bond is probably *Z*, which is more favourable with respect to the spatial proximity of  $\text{NCH}_3$  group with both the benzene rings (Fig. 2). The benzene rings are also spatially close (as follows from NOE). The structure in solution is then similar to the structure found in crystal (Fig. 7).

Due to a low natural abundance of  $^{15}\text{N}$  isotope the values of  $J(^{13}\text{C}, ^{15}\text{N})$  could be determined only for isotopically enriched compounds **3a** and **4** nevertheless similar conclusions can be made also



**Scheme 3.** Synthesis of the starting enaminones **2** and azo coupling products **3**, **4**.



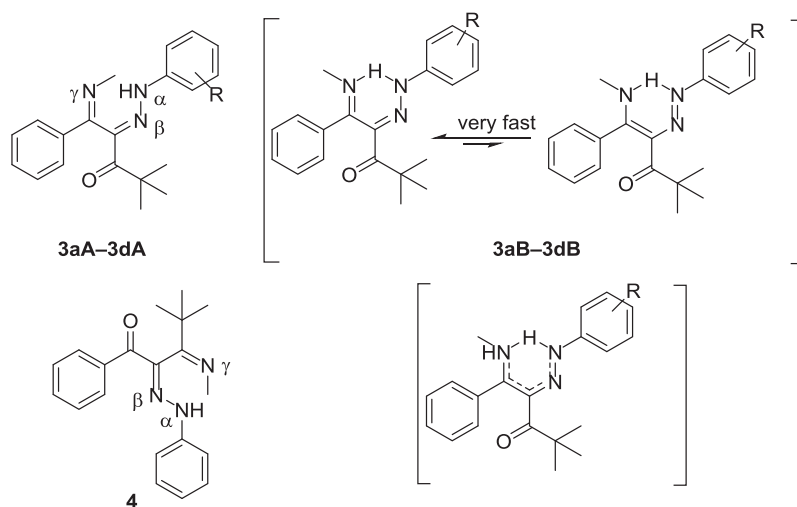
**Scheme 4.** The stereochemical dependence of  $2J(^{15}\text{N}, ^{13}\text{C})$  and the values found for compounds **3a**, **4**.

for compounds **3b–3d**. The conclusions are summarized in [Scheme 5](#).

On comparison the structures of **3a–d** and **4** and their confrontation with the previously performed studies [\[9,10,18–27\]](#) some conclusions on the influence of the structure of the enaminone on the structure of the azo coupling product can be made:

From the tautomeric point of view, compound **4** can be compared with compound **5** ([Scheme 6](#)) formed by azo coupling on 3-methylamino-1-phenylbut-2-en-1-one (4-methylphenyldiazenyl group is very similar to phenyldiazenyl group). The planar conjugated system in the molecule of **5** enables the formation of strong intramolecular hydrogen bond  $\text{N}-\text{H}\cdots\text{N}=\text{}$  and, hence, the presence of substantial amount of azo form in the tautomeric mixture (about 50%) [\[24\]](#). The molecule of **4** is distorted due to the presence of bulky *tert*-butyl group and exists as a pure hydrazone-form having intermolecular hydrogen bond  $\text{N}-\text{H}\cdots\text{O}=\text{C}$  with a carbonyl oxygen which do not participate in the tautomeric exchange.

Similar conclusions can be drawn also upon comparing the structures of azo coupling products from 2,2-dimethyl-5-methylamino-5-phenylpent-4-en-3-one **3** and 4-amino-4-phenylbut-3-en-2-one **7** [\[22\]](#). On azo coupling with benzenediazonium a mixture of two products is formed in both the cases. In the case of the products **7** both the compounds have an intramolecular hydrogen bonds  $\text{N}-\text{H}\cdots\text{N}=\text{}$  in a planar conjugated heterodiene system RAHB (Resonant Assisted Hydrogen Bonding [\[36\]](#)). The major product is a mixture of azo and hydrazo tautomers with the former prevailing. On the other hand the major form of the *tert*-butyl derivative **3** is pure hydrazone with an intermolecular



**Scheme 5.** The structure of the azo coupling products in  $\text{CDCl}_3$ .



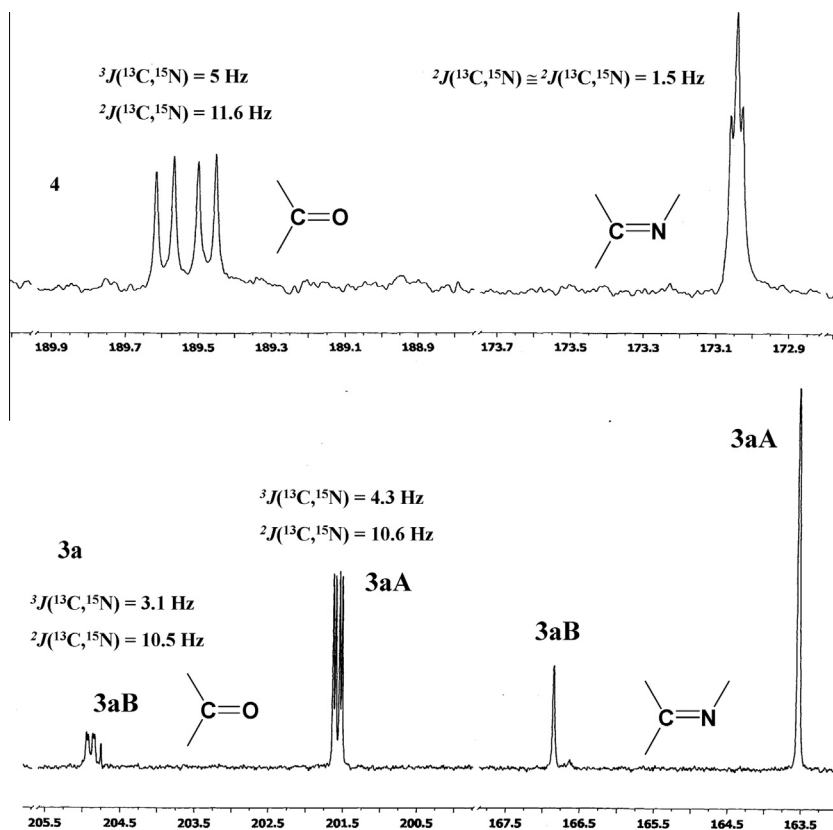


Fig. 1. Detail of  $^{13}\text{C}$  NMR spectra of compounds **3aA/3aB** and **4** with the values of  $^{15}\text{N}$ – $^{13}\text{C}$  coupling constants.

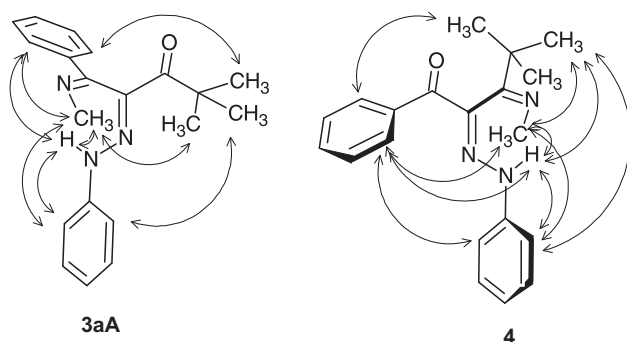


Fig. 2. NOE interactions found for compounds **3aA** and **4**.

hydrogen bond  $\text{N}-\text{H}\cdots\text{N}=\text{}$  and the minor one is a mixture of azo/hydrazo tautomers (the latter prevailing) with an intramolecular hydrogen bond. The change in the tautomeric behaviour is again induced by the presence of bulky *tert*-butyl group and thus by an impossibility of achieving the planarity of the heterodiene system.

On the basis of the findings obtained by studying the products of azo coupling to isomeric enaminones derived from benzoylacetone the following can be stated: the switching from the enaminones with primary amino group **6** to the *N*-methyl analogues **5** meant a slight (about 10%) increasing of hydrazo form (Scheme 6). The switching from **6** (with benzoyl group) to its isomer **7** (with acetyl group) meant both shift towards the hydrazone and the formation of *E/Z* isomeric mixture differing in the position of an intramolecular hydrogen bonding. The minor isomer with  $\text{C}=\text{O}\cdots\text{H}-\text{N}$  hydrogen bond, however, was pure azo compound. The shift from **7** to **3a**, i.e. from the primary amino group to *N*-methyl group and increasing the steric demands ( $\text{Me} \rightarrow t\text{Bu}$ ) has significant consequences which is a considerable shift towards hydrazo form both

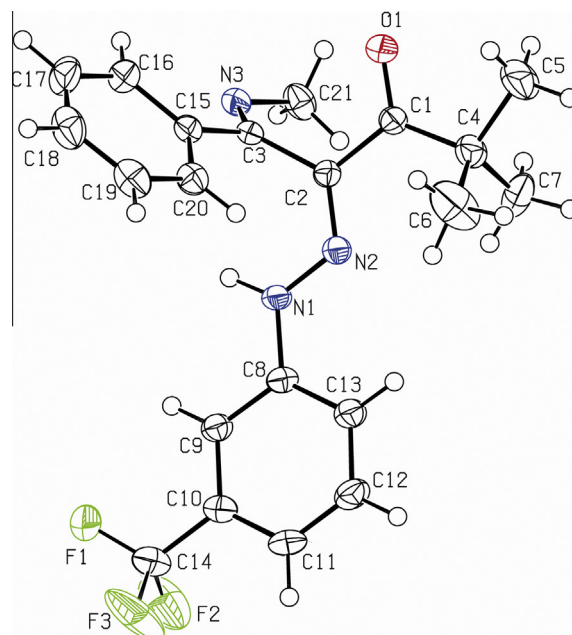
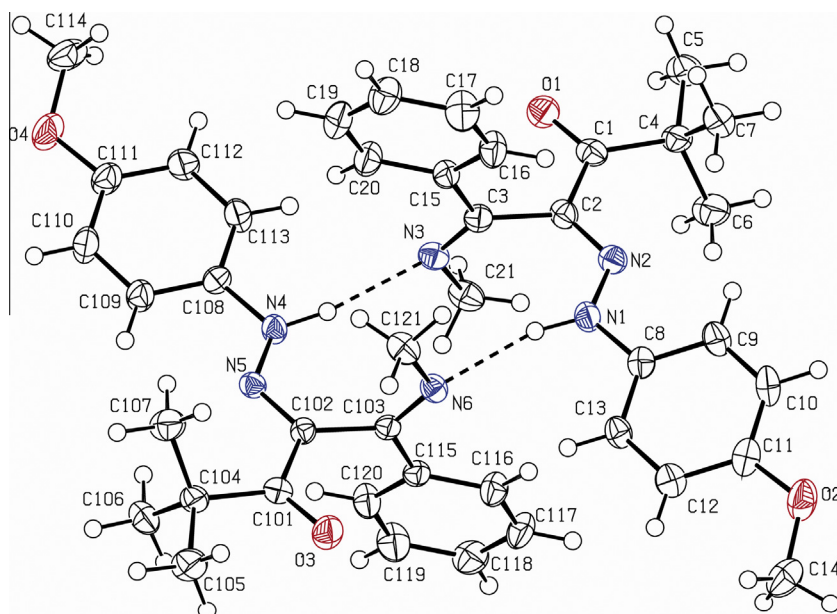


Fig. 3. The molecular structure (ORTEP 50% probability level) of **3d**. Selected interatomic distances and angles are given in Table 3.

in the major (entirely) and in minor (predominantly) forms. Another consequence is the absence of the intramolecular hydrogen bond in the major isomer (Scheme 6).

Upon comparison the compounds **3** and **4** the similar trend as in the comparison of the isomers **6** and **7** can be stated, i.e. an increasing the number of forms.



**Fig. 4.** The molecular structure (ORTEP 50% probability level) of **3c** with intermolecular hydrogen bond interaction between two independent molecules N1–H1...N6 and N4–H4...N3. Selected interatomic distances and angles are given in Table 3.

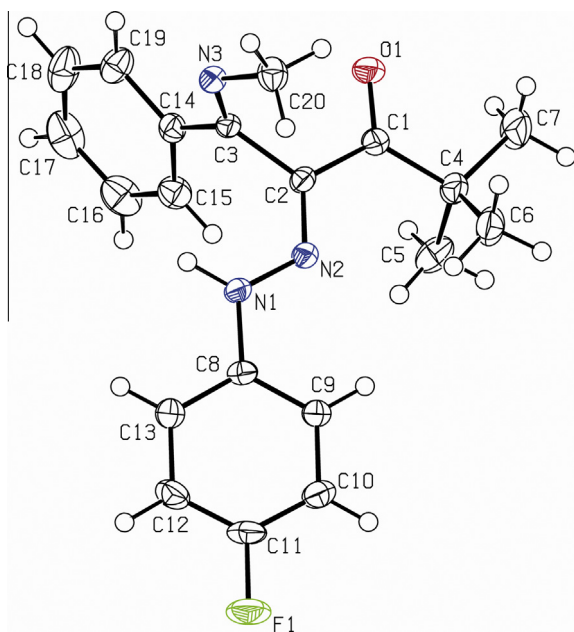


**Fig. 5.** The molecular structure (ORTEP 50% probability level) of **3b**. Selected interatomic distances and angles are given in Table 3.

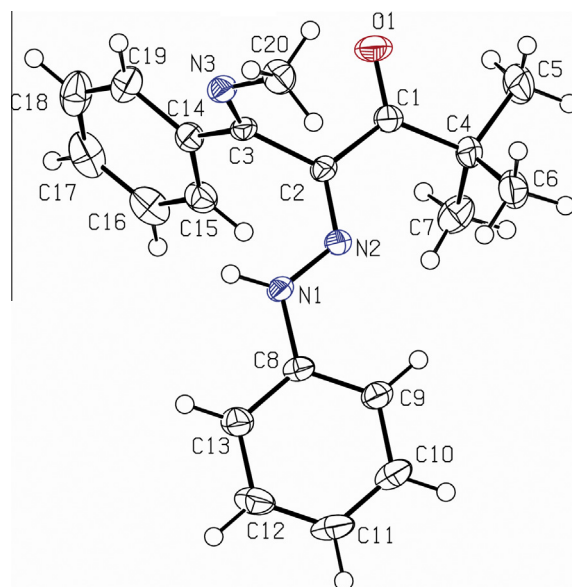


**Fig. 6.** The molecular structure (ORTEP 50% probability level) of **3a**. Selected interatomic distances and angles are given in Table 3.

### Crystallography

Selected crystallographic data, bond lengths and bond angles for **3a–d** and **4** are summarized in Tables 2–4. ORTEP diagrams of the compounds **3a–d** and **4** are in Figs. 3–6. The molecules of compounds **3a,b,d** form dimers through the intermolecular hydrogen bonds N1–H1...N6 and N4–H4...N3 like the molecules **3c** (Fig. 4). Compound **4** (Fig. 7) crystallizes in the same crystal system and space group like **3a** and **3b**, but with eight molecules within the unit cell forms chains due to intermolecular hydrogen bonds instead of dimeric structures observed for the compounds **3**.

Similarly to compounds reported previously [22,24,37] in all structures of **3a–d** a mixture of two tautomeric forms is present.

Both the enamino–diazenyl and imino–hydrazone heterodienic fragments are tautomeric systems with an extended  $\pi$ -delocalization where the tautomeric ratios cannot be determined from the analysis of the bond distances. Similarly as in the recent reports, these ratios have been calculated from the refined occupancies of both tautomeric hydrogens with partial occupancies, situated in a double well potential, obtaining, for all compounds, similar tautomeric ratios 83/17 for **3a**, 81/19 for **3d**, 78/22 for **3b**, and 69/31% for **3c**, respectively, for imino–hydrazone form. The order of the compounds in the hydrazone content is in accordance with the results obtained for  $\text{CDCl}_3$  solution. The tautomeric exchange in this case, on the contrary to all the cases having been hitherto studied [9,10,18–27], is mediated by means of intermolecular and not intramolecular exchanges of the protons between two nitrogen

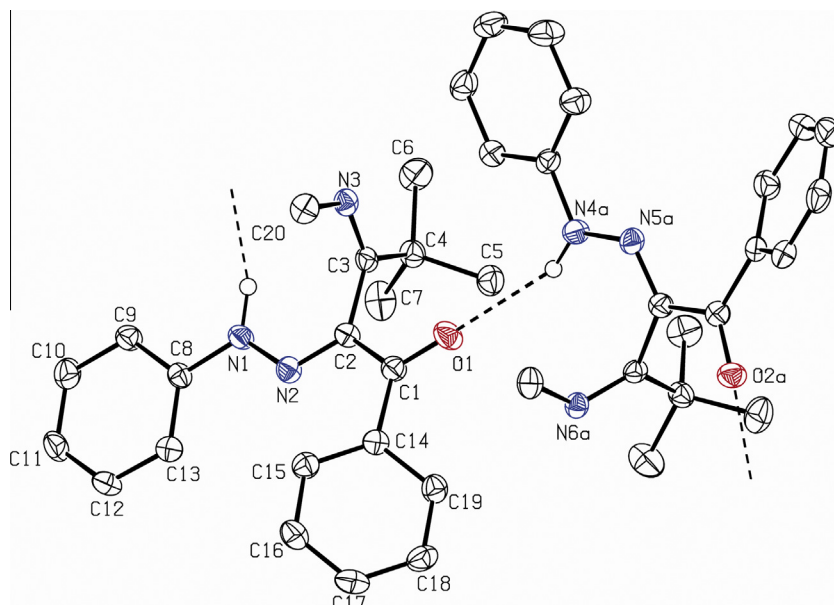
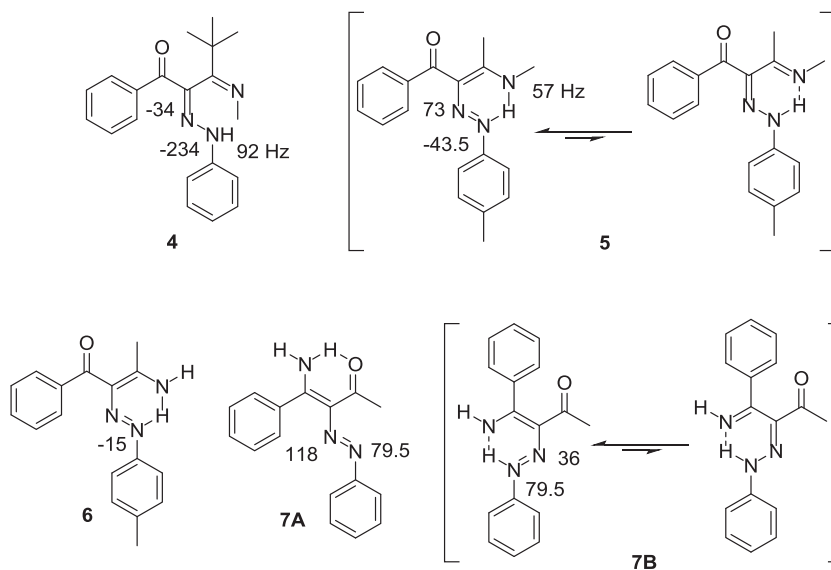


**Fig. 7.** The molecular structure (ORTEP 50% probability level) of **4** with intermolecular hydrogen bond interaction between two independent molecules  $N1-H1 \cdots O2i$  and  $N4a-H4a \cdots O1$ . Selected interatomic distances and angles are given in Table 3.



**Scheme 6.** Comparison the presently studied compounds **3**, **4** with those previously studied.

**Table 3**  
Selected interatomic distances (Å), angles (°) and interplanar angles (°) for compounds **3a–d** and **4** (parameter for the second independent molecule is given in parenthesis).

	<b>3a</b>	<b>3b</b>	<b>3c</b>	<b>3d</b>	<b>4</b>
O1–C1	1.2165(19)	1.220(2)	1.224(3) (1.223(3))	1.220(2)	1.230(2) (1.232(2))
C1–C2	1.482(2)	1.479(2)	1.476(3) (1.480(3))	1.486(2)	1.477(3) (1.478(3))
N2–C2	1.2932(18)	1.296(2)	1.299(3) (1.294(3))	1.292(2)	1.298(2) (1.302(2))
N1–N2	1.3306(18)	1.335(2)	1.333(3) (1.338(3))	1.3382(19)	1.334(2) (1.330(2))
C2–C3	1.509(2)	1.512(2)	1.511(3) (1.506(3))	1.508(2)	1.516(3) (1.508(3))
N3–C3	1.276(2)	1.277(2)	1.276(3) (1.272(3))	1.277(2)	1.269(2) (1.270(2))
O1–C1–C2	116.39(14)	116.33(15)	116.6(2) (116.9(2))	116.01(15)	118.90(18) (118.67(17))
N2–C2–C1	119.15(13)	119.97(14)	119.6(2) (119.0(2))	119.70(14)	117.82(17) (116.51(17))
N1–N2–C2	120.22(13)	119.61(14)	119.6(2) (120.08(19))	119.11(14)	119.46(17) (119.25(17))
N2–C2–C3	125.14(14)	125.00(15)	124.8(2) (124.9(2))	124.36(14)	123.47(17) (123.77(17))
N3–C3–C2	123.78(14)	123.59(15)	124.2(2) (123.1(2))	124.02(15)	122.03(18) (123.61(17))
Interplanar <sup>a</sup>	84.6(2)	85.8(2)	87.1(2) (89.0(3))	79.5(3)	89.7(3) (74.0(2))

<sup>a</sup> Interplanar angle between N2–C2–C3 (N5–C102–C103) and N3–C3–C2 (N6–C103–C102) planes.



**Table 4**  
Hydrogen interactions (Å, °).

	D—H...A	d(D...A)	<(DAH)	Symm. transformation
<b>3a</b>	N(1)—H(1)...N(3i)	3.0666(18)	173.5	−x + 1, −y, −z + 1
<b>3b</b>	N(1)—H(1)...N(3i)	3.023(2)	167.7	−x + 1, −y, −z + 2
<b>3c</b>	N(1)—H(1)...N(6)	2.975(3)	160.9	—
	N(4)—H(4)...N(3)	3.096(3)	170.9	—
<b>3d</b>	N(1)—H(1)...N(3i)	3.071(2)	165.4	−x + 1, −y, −z + 1
<b>4</b>	N(4)—H(4)...N(6)	3.215(2)	117.2	—
	N(4)—H(4)...O(1i)	3.345(2)	155.4	−x + 1, −y, −z
	N(1)—H(1)...O(2i)	3.293(2)	149.1	−x, −y, −z

atoms. On the other hand the polymeric structure of **4** made via hydrogen bonds N—H...O= (Fig. 7) reveals similar interatomic distances with a conjugated character but retains strictly in the imino-hydrazo-carbonyl tautomeric form in the solid state, just as in the CDCl<sub>3</sub> solution. The conformation of the molecule prevents from the formation of the N—H...N= hydrogen bond necessary for the imino-hydrazo – enamino-azo tautomeric exchange. This is the major difference between the compound **4** and all the azo coupled enamines having been studied so far [9,10,18–27]. The carbonyl does not participate in the tautomeric exchange.

Separations between donor and acceptor atoms involved in such a H-bond is much longer in cases of **3a–d** and **4** (see Table 4) than in analogous compounds described in the literature (2.565(1)–2.639(3) Å) which could be explained by hydrogen bonds assisted by resonance concept (RAHB) [36,38–40] available for compounds where a six membered heterocyclic ring is formed by a H-bond [22,24,37].

The planes where atoms N2–C2–C3 and N3–C3–C2 or N5–C102–C103 and N6–C103–C102 respectively are located in the molecules **3a–d** and **4** (Figs. 3–6) make an interplanar angle close to 90° in all the cases (Table 3). It means that the conjugation between the methylimino and hydrazono groups does not exist. Consequently, the bond C2–C3 or C102–C103 respectively has the length characteristic for a single bond (1.506–1.516 Å) on the contrary to the previously studied cases where this bond had, due to the conjugation and tautomerism, length 1.408–1.430 Å. This bond is even longer than the corresponding one in the compounds existing solely in the imino-hydrazono tautomeric form (*Csp*<sup>2</sup>–*Csp*<sup>2</sup> ca 1.484 Å, Ref. [22]).

## Conclusions

An introduction of *tert*-butyl group into the molecule of enamines has a significant impact on the structure of their reaction products with diazonium tetrafluoroborates. For the first case it has been observed that the azo coupled enamines with *N*-alkyl group exist in CDCl<sub>3</sub> solution predominantly or even solely as hydrazones. Only a minor portion of these molecules (**3aB–3dB**) is capable of forming an intramolecular hydrogen bond N—H...N and, hence, undergoing azo-hydrazone tautomerism in solution. The major part of the compounds exists as pure hydrazone form. In solid state the intramolecular hydrogen bonding does not manifest at all and the tautomeric equilibrium is mediated probably via intermolecular N—H...N interactions. If the compound is not capable of this interaction, it exists as the pure hydrazone form also in solid state. This is the case of the compound **4**. The position of the tautomeric equilibrium is affected by the substituents (coming from the starting diazonium salt) present in the molecule of the azo coupling product. Amount of the hydrazone increases in the order 4-OMe < 4-F < 3-CF<sub>3</sub> < H, both in solution and in solid state.

## Appendix A. Supplementary material

Crystallographic data for structural analysis have been deposited with the Cambridge Crystallographic Data Centre, CCDC Nos. 983844, 942937, 942938, 942936 and 983845 for **3a–d** and **4** respectively. Copies of this information may be obtained free of charge from The Director, CCDC, 12 Union Road, Cambridge CB2 1EY, UK (fax: +44 1223 336033; e-mail: deposit@ccdc.cam.ac.uk or www: <http://www.ccdc.cam.ac.uk>). Supplementary data associated with this article can be found, in the online version, at <http://dx.doi.org/10.1016/j.molstruc.2014.06.069>.

## References

- [1] V. Bekárek, K. Rothschein, P. Vetešník, M. Večeřa, *Tetrahedron Lett.* 9 (1968) 3711–3713.
- [2] V. Bekárek, I. Dobáš, J. Socha, P. Vetešník, M. Večeřa, *Coll. Czech. Chem. Commun.* 35 (1970) 1406–1414.
- [3] A. Lyčka, D. Šnobl, V. Macháček, M. Večeřa, *Org. Magn. Reson.* 15 (1981) 390–393.
- [4] A. Lyčka, D. Šnobl, V. Macháček, M. Večeřa, *Org. Magn. Reson.* 16 (1981) 17–19.
- [5] A. Lyčka, *Annu. Rep. NMR Spectrosc.* 42 (2000) 1–57.
- [6] R. Marek, A. Lyčka, *Curr. Org. Chem.* 6 (2002) 35–66.
- [7] H. Zollinger, *Color chemistry, syntheses, properties, and applications of organic dyes and pigments*, third ed., *Selected Properties of Azo Compounds*, Wiley, Weinheim, 2001. p. 192 (Chapter 7.5).
- [8] A. Lyčka, *Collect. Czech. Chem. Commun.* 47 (1982) 1112–1120.
- [9] V. Macháček, A. Lyčka, P. Šimůnek, T. Weidlich, *Magn. Reson. Chem.* 38 (2000) 293–300.
- [10] P. Šimůnek, V. Bertolasi, M. Pešková, V. Macháček, A. Lyčka, *Org. Biomol. Chem.* 1 (2003) 3250–3256.
- [11] I. Sheikshoae, W.M.F. Fabian, *Curr. Org. Chem.* 13 (2) (2009) 149–171.
- [12] E. Kolehmainen, B. Osmialowski, *Int. Rev. Phys. Chem.* 31 (4) (2012) 567–629.
- [13] L.J.O. Figueiredo, C. Kascheres, *J. Org. Chem.* 62 (4) (1997) 1164–1167.
- [14] J. March, *Advanced organic chemistry*, fourth ed., *Reactions, Mechanisms and Structure*, Wiley, New York, USA, 1992. p. 593.
- [15] M.B. Smith, *March's advanced organic chemistry*, seventh ed., *Reactions, Mechanisms and Structure*, Wiley, New York, USA, 2013. p. 675.
- [16] F.R. Japp, F. Klingemann, *Ber.* 20 (1887) 3284–3286.
- [17] F.R. Japp, F. Klingemann, *Ber.* 20 (1887) 3398–3401.
- [18] V. Kettmann, J. Lokaj, P. Šimůnek, V. Macháček, *Acta Cryst. C* 57 (2001) 737–739.
- [19] P. Šimůnek, A. Lyčka, V. Macháček, *Eur. J. Org. Chem.* 16 (2002) 2764–2769.
- [20] P. Šimůnek, V. Bertolasi, V. Macháček, *J. Mol. Struct.* 64 (2002) 41–52.
- [21] P. Šimůnek, V. Bertolasi, A. Lyčka, V. Macháček, *Org. Biomol. Chem.* 1 (2003) 3250–3256.
- [22] P. Šimůnek, V. Bertolasi, M. Pešková, V. Macháček, A. Lyčka, *Org. Biomol. Chem.* 3 (2005) 1217–1226.
- [23] P. Šimůnek, L. Lusková, M. Svobodová, V. Bertolasi, A. Lyčka, V. Macháček, *Magn. Reson. Chem.* 45 (2007) 330–339.
- [24] P. Šimůnek, M. Svobodová, V. Bertolasi, L. Pretto, A. Lyčka, V. Macháček, *New J. Chem.* 31 (2007) 429–438.
- [25] V. Macháček, V. Bertolasi, P. Šimůnek, M. Svobodová, J. Svoboda, E. Černošková, *Cryst. Growth Des.* 10 (2010) 85–91.
- [26] P. Šimůnek, V. Macháček, *Dyes Pigm.* 86 (2010) 197–205.
- [27] P. Šimůnek, V. Bertolasi, V. Macháček, *Eur. J. Org. Chem.* (2013) 5683–5691.
- [28] P. Šimůnek, M. Svobodová, V. Macháček, *J. Heterocycl. Chem.* 46 (2009) 650–655.
- [29] Z. Otwinowski, W. Minor, *Methods in enzymology. Processing of X-ray diffraction data collected in oscillation mode* 276 (1997) 307–326.
- [30] P. Coppens, in: F.R. Ahmed, S.R. Hall, C.P. Huber (Eds.), *Crystallographic Computing*, Munksgaard, Copenhagen, 1970. pp. 255–270.
- [31] A. Altomare, G. Cascarano, C. Giacovazzo, A. Guagliardi, *J. Appl. Crystallogr. (Early Finding of Preferred Orientation – A New Method)* 27 (1994) 1045–1050.
- [32] G.M. Sheldrick, *SHELXL-97*, University of Göttingen, Göttingen, 2008.
- [33] A. Lyčka, *Collect. Czech. Chem. Commun.* 13 (1980) 3354–3359.
- [34] H.-O. Kalinowski, S. Berger, *Carbon-13 NMR Spectroscopy*, Wiley, Chichester, 1988. p. 573.
- [35] G.W. Buchanan, B.A. Dawson, *Org. Magn. Reson.* 13 (1980) 293–298.
- [36] P. Gilli, V. Bertolasi, V. Ferretti, G. Gilli, *J. Am. Chem. Soc.* 122 (2000) 10405.
- [37] P. Gilli, V. Bertolasi, L. Pretto, A. Lyčka, G. Gilli, *J. Am. Chem. Soc.* 124 (2002) 13554–13567.
- [38] G. Gilli, F. Bellucci, V. Ferretti, V. Bertolasi, *J. Am. Chem. Soc.* 1023 (1989) 111.
- [39] G. Gilli, P. Gilli, *J. Mol. Struct.* 552 (2000) 1.
- [40] V. Bertolasi, P. Gilli, V. Ferretti, G. Gilli, *Acta Crystallogr., Sect. B* 50 (1994) 617.